Cuadernos de Investigación Geográfica *Geographical Research Letters*	2022	Nº 48	pp. 59-78	EISSN 1697-9540

http://doi.org/10.18172/cig.5098

IDENTIFICATION OF DESERTIFIED AND PRESERVED AREAS IN A CONSERVATION UNIT IN THE STATE OF PARAÍBA - BRAZIL

LEANDRO F. DA SILVA[1], BARTOLOMEU I. SOUZA[1], RAFAEL CÁMARA ARTIGAS[2]*

[1]Dept. Geography, University of Paraíba, Brazil.

[2]Dept. Physical Geography and Regional Geographic Analysis, University of Seville, Spain.

ABSTRACT. The objective of this study is to identify and analyse the main characteristics of areas potentially degraded by desertification and of preserved areas using the Soil Surface Moisture Index (SSMI), alongside the Land Surface Temperature (LST) and Normalized Difference Vegetation Index (NDVI). The study is based on a set of points obtained in the field and from the RGB false colour image for the Environmental Protection Areas (EPA) of the Cariri, in the semi-arid region of Paraíba, using a space-time cross-section covering both rainy and dry periods. The results showed that at all points in Desertified Areas, the main characteristics were a low SSMI, high LST and low NDVI in both periods. The Preserved Areas, on the other hand, presented a high SSMI, moderate LST and high NDVI in the rainy period, with the same characteristics repeated in the dry period for SSMI and NDVI, but with a low LST. Timely identification of these characteristics, both in areas degraded by desertification and in better preserved areas, can provide useful information for future decisions relating to the physical and territorial management of the Conservation Unit.

Identificación de áreas desertificadas y preservadas en una unidad de conservación en el Estado de Paraíba - Brasil

RESUMEN. El objetivo de este estudio fue identificar y analizar las principales características de áreas potencialmente degradadas por desertificación y de áreas preservadas. Para ello se utilizaron el Índice de Humedad Superficial del Suelo (IHSS), junto con la Temperatura de la Superficie de la Tierra (TS) y el Índice de Vegetación de Diferencia Normalizada (IVDN). El estudio está basado en un conjunto de puntos obtenidos en el campo y en la composición de la imagen de falso color RGB para el Área de Protección Ambiental (APA) del Carirí, en la región semiárida de Paraíba, utilizando un corte espacio-temporal que abarca la estación lluviosa y seca. Los resultados mostraron que en todos los puntos de las Áreas Desertificadas las principales características fueron el IHSS bajo, TS alto y IVDN bajo en ambos períodos. Las Áreas Preservadas, por su parte, presentaron IHSS alto, TS moderado e IVDN alto en la época de lluvias, con las mismas características repetidas en el periodo seco para IHSS y IVDN, pero con TS bajo. La identificación puntual de estas características, tanto en áreas degradadas por desertificación como en las más conservadas, puede aportar información útil para la toma de decisiones futuras relacionadas con la gestión territorial y física de la Unidad de Conservación.

Key words: Desertification, Carirí EPA, SSMI.

Palabras clave: Desertificación, APA del Carirí, IHSS.

Received: 4 Mayo 2021

Accepted: 6 October 2021

*Corresponding author: Rafael Cámara Artigas. Dept. Physical Geography and Regional Geographic Analysis, University of Seville, Spain. E-mail address: rcamara@us.es

1. Introduction

Brazil has the second highest proportion of dry forests degraded by human activity of all the countries in the Americas (Portillo-Quintero and Sánchez-Azofeifa, 2010). Among Brazil's different ecosystems, the Caatinga, which is the dominant biome in the Brazilian Northeast, is one of the most threatened and disrupted. The main threats to this ecosystem are the illegal extraction of wood for energy and for producing fences, as well as the expansion of farming, which has created large areas of desertified land (Castelletti *et al.,* 2003) and has even affected the Conservation Units (CU) created by the state.

These CUs are defined by the Brazilian Ministry of the Environment (MMA) as territorial units with noteworthy natural characteristics, which serve to ensure the representation of important, ecologically viable samples of the different populations, habitats and ecosystems present in the country and to preserve the existing biological heritage (MMAUC, 2020).

These areas allow traditional, sustainable, rational use of natural resources to continue, with special rules and regulations in place for local communities to engage in sustainable economic activity. They are created in law by the federal, state and municipal governments after technical studies are carried out on the areas of land in question and local people consulted where necessary (MMAUC, 2020).

CUs in Brazil are divided into two main categories: 1) Fully Protected and 2) Sustainable Use. The latter includes the country's Environmental Protection Areas or EPAs (MMAUC, 2020), where people can make direct use of natural resources, albeit in a carefully controlled manner.

Desertification is defined by the United Nations (UN) as the reduction or destruction of biological potential, starting with alterations to natural vegetation by human intervention in arid, semi-arid and dry sub-humid regions. These processes are exacerbated by climatic fluctuations (MMA, 2020).

In 1994, the UN oversaw the drafting of a global plan to tackle desertification and the effects of drought by adopting effective measures at all levels, based on cooperation agreements and international collaboration (MTERD, 2020). Nevertheless, many of the countries affected by the issue, including Brazil, have been slow to take action and their measures have had little practical impact.

According to data from the National Semi-Arid Institute (INSA, 2015)) in Brazil, the area of the country susceptible to desertification covers 1,340,863km² and includes 1,488 municipalities in nine states in the semi-arid region in the Brazilian Northeast. The main hotspots for desertification in Brazil's semi-arid region are: Seridó in the states of Rio Grande do Norte and Paraíba; Cariris Velhos in Paraíba; Inhamuns in Ceará; Gilbués in Piauí; Sertão Central in Pernambuco; and Sertão do São Francisco in Bahía. These areas are the product of inadequate or non-existent measures to mitigate the interaction between productive activity and the natural resources available in an ecologically fragile environment (INSA, 2015). However, there is still a lack of knowledge of these degrading processes and their extent, and constant updates of this knowledge are required (INSA, 2015).

A significant proportion of the damage to natural resources, especially plant cover, is the result of people in regions at risk of desertification seeking to provide for their basic needs. Other causes include commercial agriculture and excessive demand for raw materials for industrial use (Zhou *et al.,* 2015; Bezerra *et al.,* 2020).

The impacts of this overexploitation can be seen in escalating soil erosion, especially sheet erosion, and in processes of salinisation in both irrigated agricultural land and non-irrigated land (MMA, 2020).

In desertified areas, vegetation is sparse with many dwarf plants and low levels of diversity (MMA, 2020). Therefore, desertification has a severe social and economic impact and is considered to be one of the most significant environmental issues facing the world at this time (Nascimento, 2015; Bezerra *et al.,* 2020).

In the Cariris Velhos region, Paraíba, Brazil, the desertification process is very acute and is related primarily to i) geoecological predisposition or the unstable balance resulting from climatic, edaphic and topographic factors; and ii) different types of direct or indirect human activity, which begin with the removal or degradation of plant cover (Sobrinho, 1982; MMA, 2020).

Given these characteristics, a wide range of studies have sought to address the issue in this region specifically (Souza *et al.,* 2009; Souza *et al.,* 2015a; Lemos *et al.,* 2020). As this type of degradation progresses, it is increasingly important to understand the causes in order to develop alternative measures and solutions to mitigate the problem and attempt to slow its advance.

With this in mind, current technologies can make a significant contribution to studies of desertification and have already been used in research on the issue from a wide variety of disciplines (Sousa *et al.,* 2012; Vieira *et al.,* 2020).

In recent years, the number of methods drawing on computational techniques to identify and situate environmental phenomena has also increased, using tools such as remote sensing and geotechnologies applied specifically to arid and semi-arid environments around the world.

These methods are based on bio-geophysical parameters obtained via a series of freely available sensors, such as MODIS (Moderate-resolution Imaging Spectroradiometer) on the Terra and Aqua satellites, and TM (Thematic Mapper) and OLI (Operational Land Imager) on the Landsat satellites, which are mostly used to analyse parameters such as land surface temperature (Sousa *et al.,* 2015b; Santos *et al.,* 2020) and different vegetation indices, including the traditional NDVI - Normalized Difference Vegetation Index and the SAVI - Soil-Adjusted Vegetation Index (Aquino *et al.,* 2012; Silva Filho *et al.,* 2020).

Other techniques and methodologies have been used to perform important tasks such as quantifying and situating the influence of moisture on the soil. Some of these allow the surface retention capacity, infiltration, evaporation, influence on vegetation and desertification to be estimated, as in studies conducted by Lopes *et al.* (2011), Francisco *et al. (*2017) and Inocêncio *et al.* (2020), based on the interactions between the different indices and bio-geophysical parameters obtained via remote sensing.

Against this backdrop, this study aimed to identify and analyse the main characteristics of areas potentially degraded by desertification and preserved areas in a Conservation Unit (CU) for sustainable use, located in the semi-arid region of Paraíba, Brazil, using the Soil Surface Moisture Index (SSMI) proposed by Lopes *et al. (*2011), the land surface temperature (LST) and the Normalised Difference Vegetation Index (NDVI).

2. Methodology

2.1. Study area

The Cariri EPA is situated between the municipalities of Boa Vista, Cabaceiras and São João do Carirí, between the latitudes 07º20’00” and 7º25’00” S and the longitudes 36º25’00” and 36º15’00” O, as shown in Figure 1.

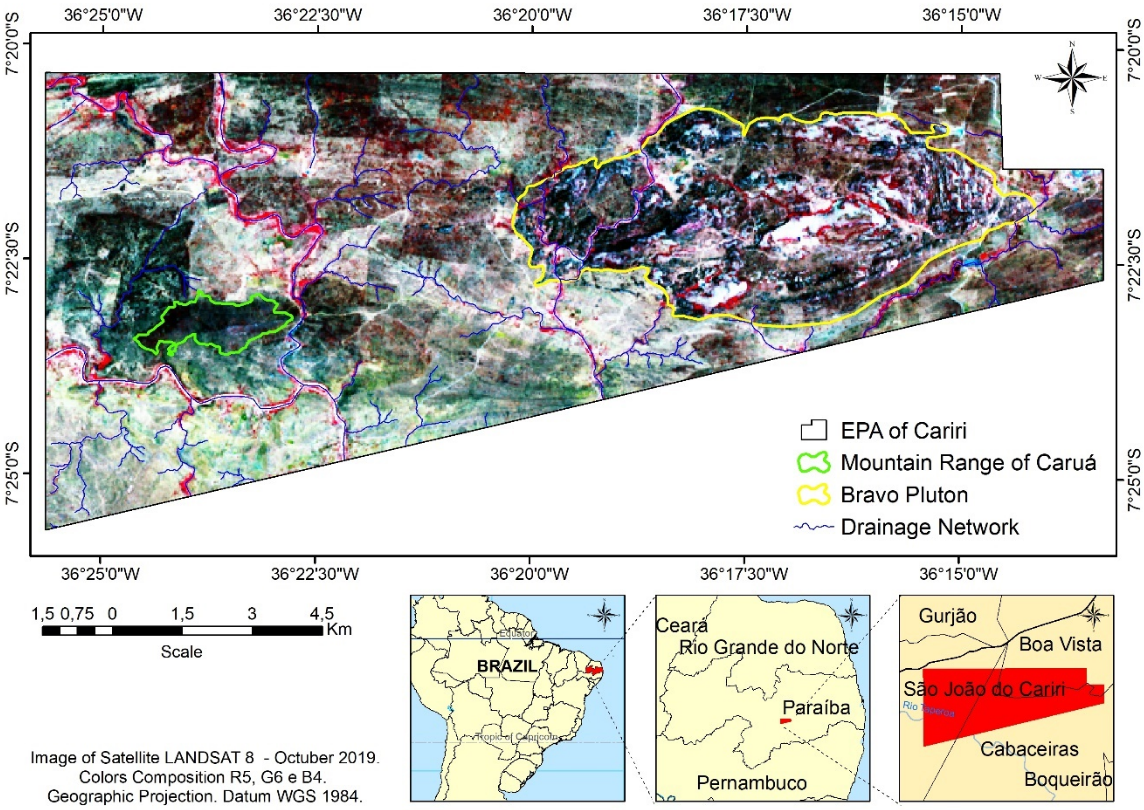

Figure 1. Map showing the location of the Cariri EPA and the areas with the most extensive plant cover in this CU.

The Cariri EPA is located in the micro-region of Cariris Velhos in the state of Paraíba, Northeast Brazil. This CU for sustainable use was created by the Secretariat of Environment in the State of Paraíba under State Decree 25083 of 8 June 2004 and covers an area of approximately 156 km².

The predominant vegetation in the region is Caatinga, which comprises a variety of physiognomies ranging from tree and shrub formations dominated by xerophilous deciduous species, as well as cacti and bromeliads (Ballén *et al.,* 2016; Souza and Souza, 2016; Lima *et al.,* 2017). Some sectors are characterised by differentiated vegetation, comprising species from humid and sub-humid areas of other Brazilian biomes. These are referred to here as Exceptional Areas and their soils and topography result in locally higher water levels, differentiating them from surrounding areas. This can be seen on varying scales across the interior of Northeast Brazil (Melo, 1988; Mello Neto *et al.,* 1985).

The climate in the region is classified by Koppen (1931) as semi-arid (BSh) or dry semi-arid, with low rainfall averaging between 400 mm and 500 mm a year (AESA, 2020a) and an average annual temperature ranging from 25 to 27°C, making this the driest region in Brazil (Souza *et al.,* 2009; Silva *et al.,* 2019a).

The main soil types found in the region are Regolith Neosol, Litholic Neosol and Chromic Luvisol, as well as Fluvic Neosol on floodplains (Ballén *et al.,* 2016; Silva *et al.,* 2019a).

From a geological perspective, the region is made up of granite rock with large rocky outcrops commonly known as *lajedos* (Lages *et al.,* 2013); one of the most prominent outcrops in this area is the Bravo Pluton, an ellipsoidal stock formed by granitic orthogneisses with a high metamorphic content (Romano *et al.,* 2018). Its surface is ellipsoidal, measuring almost 12 km long and 5 km wide (Sousa and Xavier, 2017), emerging in the centre-east of Paraíba between the municipalities of Cabaceiras and Boa Vista (Romano *et al.,* 2018).

In this CU, the most common landforms have a convex, tabular topography. The highest topographies are linked to the large rocky outcrops in the Bravo Pluton region to the West (W), with small mountain groups to the East (E) such as the Caruá Mountains, where elevations exceed 600m (Fig. 2).

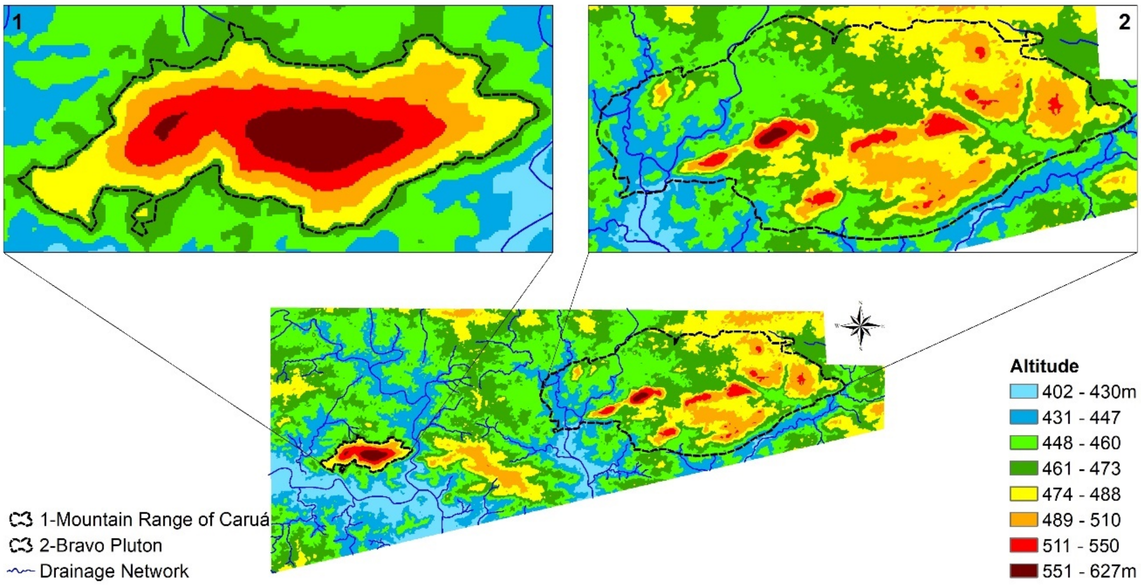

Figure 2. Map of Altitude.

2.2. Methodological procedures

The images used were produced by the Landsat 8 – OLI satellite in April (rainy period) and October (dry period) 2019 and geometrically corrected at the Q1 level (l1T) to all multispectral bands, including band 10 in the thermal infrared region, the TIR (thermal infrared sensor), orbit 215 point 065, freely available from the United States Geological Survey via USGS Earth Explorer.

The multispectral images then underwent radiometric correction and were loaded one by one into the ENVI 5.3 software in MTL format. Using the Radiometric Calibration tool, the correction algorithm was applied simultaneously to all bands. Once they had all been radiometrically corrected, the bands underwent atmospheric correction using the FLAASH Atmospheric Correction tool, which employs one of the most advanced algorithms for this type of correction: Moderate Resolution Atmospheric Transmission or MODTRAN. Using the same tool, a series of parameters were set: the type of sensor was set to OLI, the Tropical category was defined for the atmospheric model, the Rural category was set for the aerosol model, 2-band (K-T) was set for aerosol retrieval and 40km for the initial visibility.

The next step was to normalise the corrected atmospheric images, automatically balancing the levels of each pixel by applying a Gaussian function using the Band Math tool in ENVI 5.3.

2.2.1. Land Surface temperature (LST)

To obtain the land surface temperature (LST), thermal infrared band 10 (B10) from the TIRS sensor with a spectral range of 10.6 -11.19 µm was used for both months, with three key steps required:

I. conversion of the grey levels of the thermal band into spectral radiance, via the following equation (eq. 1):

$$L_\lambda = \left(\frac{L\max_\lambda - Lmin_\lambda}{Q_{\text{cal max}} - Q_{\text{cal min}}}\right) * (Q_{cal} - Q_{\text{cal min}}) + L_{min\lambda} \qquad \text{eq. 1}$$

Where: L_λ= spectral radiance ($W/m^2M.^{1}\cdot\mu m^{1}$); Q_{cal}= quantified pixel value and digital level calibration (DN); Q_{calmin} = minimum value of pixel levels (DN = 1); Q_{calmax}= maximum value of pixel levels (DN = 255); $L_{min\lambda}$= minimum spectral radiance (1.238 W/ m^2 sr^1 μm^1); $L_{max\lambda}$= maximum spectral radiance (15.303 W/ m^2 sr^1 μm^1).

II. conversion of radiance values into temperature, represented in degrees Kelvin (K), via the following equation (eq. 2):

$$\text{LST} = \frac{K_2}{ln\,(K_1/L_\lambda + 1)} \qquad \text{eq. 2}$$

Where: LST= land surface temperature; ln= constant of the equation; L_λ= spectral radiance (result of eq.1); K_1= calibration constant 1 (607.76 W/ m^2 sr^1 μm^1); K_2= calibration constant 2 (1260.56 W/ m^2 sr^1 μm^1).

The calibration constants (K_1 and K_2) used were obtained from the metadata (MTL) file in the information package for the bands provided when downloading images from the USGS website.

III. conversion of the ST in degrees Kelvin (K) to degrees Celsius (C), via the following expression (exp.1):

$$ST_{°C} = ST_K - 273.15 \qquad \text{exp. 1}$$

Where: $ST_{°C}$= surface temperature in Celsius; ST_K= surface temperature in Kelvin (result of equation 2); 273.15= temperature equivalent to 0° degrees Celsius.

The following tools were used for these three steps: ArcToolbox – Spatial Analyst Tools – Map Algebra – Raster Calculator in ArcGIS 10.3.

2.2.2. Normalised Difference Vegetation Index (NDVI)

The Normalised Difference Vegetation Index (NDVI) was proposed by Rouse *et al. (*1973) and is obtained via the equation (eq. 3.):

$$NDVI = \frac{\rho_{NIR} - \rho_{RED}}{\rho_{NIR} + \rho_{RED}} \qquad \text{eq. 3}$$

Where: ρNIR= near-infrared reflectance; ρRED= red reflectance

The values vary from -1, which indicates an absence of vegetation, to 1, which shows maximum vegetation. This process used the red (B4) and near-infrared (B5) bands corrected for two months. ArcGis 10.3 software was then used and equation 3 applied via the following tools: ArcToolbox - Spatial Analyst Tools - Map Algebra - Raster Calculator.

2.2.3. Soil Surface Moisture Index (SSMI)

The Soil Surface Moisture Index (SSMI) was initially suggested by Zhan *et al.* (2004) and adjusted by Wang *et al.* (2010) for semi-arid regions in China. It was subsequently adapted by Lopes *et al.* (2011) for the semi-arid region in Brazil. The index considers biophysical and geophysical parameters from remote sensing, like the LST and NDVI, and consists of three steps:

I. application of the SSMI calculation to the LST values obtained (Zhan *et al.,* 2004; Lopes *et al.,* 2011), via equation 4 (eq. 4):

$$SSMI_{LST} = \frac{LST_{max} - LST}{LST_{max} - LST_{min}} \quad \text{eq. 4}$$

Where: $SSMI_{LST}$= moisture index calculated directly from LST; LST= land surface temperature; LST_{min}= minimum ST value; LST_{max}= maximum ST value.

II. application of the SSMI calculation adjusted to NDVI (Wang *et al.,* 2010; Lopes *et al.,* 2011) via equation 5 (eq. 5):

$$SSMI_{NDVI} = 1 - \left(\frac{NDVI_{max} - NDVI}{NDVI_{max} - NDVI_{min}}\right) \quad \text{eq. 5}$$

Where: $SSMI_{NDVI}$= moisture index calculated directly from NDVI; NDVI= normalised difference vegetation index; $NDVI_{min}$= minimum NDVI value; $NDVI_{max}$= maximum NDVI value.

Constant 1 relates to the reversal of values as the higher the NDVI value, the higher the soil surface moisture level (Wang *et al.,* 2010; Lopes *et al.,* 2011).

III. The last calculation is then applied to obtain the final SSMI (Lopes *et al.,* 2011), using the average SSMI generated from the relationship between the SSMILST and the SSMINDVI, via equation 6 (eq. 6):

$$SSMI = \frac{SSMI_{LST} + SSMI_{NDVI}}{2} \quad \text{eq. 6}$$

Where: SSMI= soil surface moisture index; $SSMI_{LST}$= moisture index calculated directly from LST; $SSMI_{NDVI}$= moisture index calculated directly from NDVI.

The final SSMI displays values ranging from 0 for drier surfaces to 1 for damper surfaces (Zhan *et al.,* 2004; Wang *et al.,* 2010; Lopes *et al.,* 2011).

All calculations for this step were carried out using ArcGis 10.3 and the tools ArcToolbox - Spatial Analyst Tools - Map Algebra - Raster Calculator.

2.2.4. Fieldwork and analysis

The fieldwork was carried out using a GNSS receiver at the collection points. The landscape at each collection point was also described, with particular reference to the use and occupation of the land over time. Images were recorded using a camera. Fieldwork was carried out in May and June 2018 (rainy period) and November 2019 (dry period), covering a large proportion of the Cariri EPA.

Back in the office, the points collected in the field with coordinates from the UTM map used for reference were converted individually to Shapefile format before being separated into two categories for analysis: 1) Desertified areas and 2) Preserved areas.

Eleven real points (RP) were obtained for Desertified Areas, which were made up of open shrubby Caatinga at different stages of degradation, and fourteen points were obtained for Preserved Areas, comprising closed shrubby arboreal Caatinga and areas of differentiated vegetation referred to here as Exceptional Areas.

The field information relating to the points in the Desertified Areas was classified according to the intensity of desertification following the system proposed by Conti (2007) and organised by Araújo and Lima (2019), as shown in Table 1.

The 11 points obtained in the field fell into two desertification categories—slight and moderate—as shown in Table 1. Therefore, the term Desertified Areas was used for all points with these characteristics in this study.

Table 1. Intensity of desertification.

Classification	Characteristics
Slight	Minor deterioration of plant cover and soil.
Moderate	Significant deterioration of plant cover and appearance of sand nodules. Evidence of salinisation of soils and formation of gullies and holes.
Severe	Significant expansion of areas prone to gullies and appearance of sand. Expansion of wind erosion. Increase in ruts and holes in the soil.
Very severe	Almost complete disappearance of biomass. Sealing and intense salinisation of soils.

Source: Conti (2007); Araújo and Lima (2019b).

To increase and equalise the number of points to be analysed for each category and ensure greater representation of the areas which were not monitored during fieldwork in particular, the points obtained from the false colour images were added between bands B4, R6 and G5 for each period, according to the characteristics of the real points (Table 2).

Table 2. Characteristics of the real points (RP) in the false colour images B4, R6 and G5.

Real Points	**Colour**				**Texture**	**Shape**
Period	Rainy		Dry		Rainy/Dry	Rainy/Dry
Desertified Areas	White, Light Green and Cyan		White, Brown and Cyan	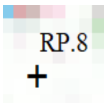	Smooth, not very rough	Regular and Irregular
Preserved Areas	**Colour**				**Texture**	**Shape**
Period	Rainy		Dry		Rainy/Dry	Rainy/Dry
Shrubby arboreal Caatinga	Red and Black		Dark Green and Black		Smooth, not very rough	Irregular
Exceptional Areas	Red	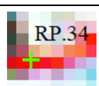	Dark Red		Smooth, not very rough	Rectangular, Thin and Irregular

Source: Compiled by the authors using data from the Landsat 8 OLI satellite - bands B4, R6 and G5 – USGS Explorer 2019.

The points obtained from the images, based on the characteristics of the real points, were labelled IP, taking into account aspects such as the colour, texture and shape of both categories. In this way, 15 points were obtained for Desertified Areas (IP.11-IP.25) and 11 points for Preserved Areas (IP.40-IP.50), which were added to the real points (RP) to produce a total of 50 points (Table 3) for analysis.

Table 3. Final points.

Desertified Areas	Preserved Areas
RP.1 – RP.10	RP.26 – RP.39
IP.11 – IP.25	IP.40 – IP.50

3. Results and discussion

3.1. Land Surface Temperature (LST) and Normalised Difference Vegetation Index (NDVI)

The first results obtained were the LST and NDVI values, which were calculated and then described for the entire Cariri EPA during the two periods analysed (rainy and dry), as shown in Figure 3.

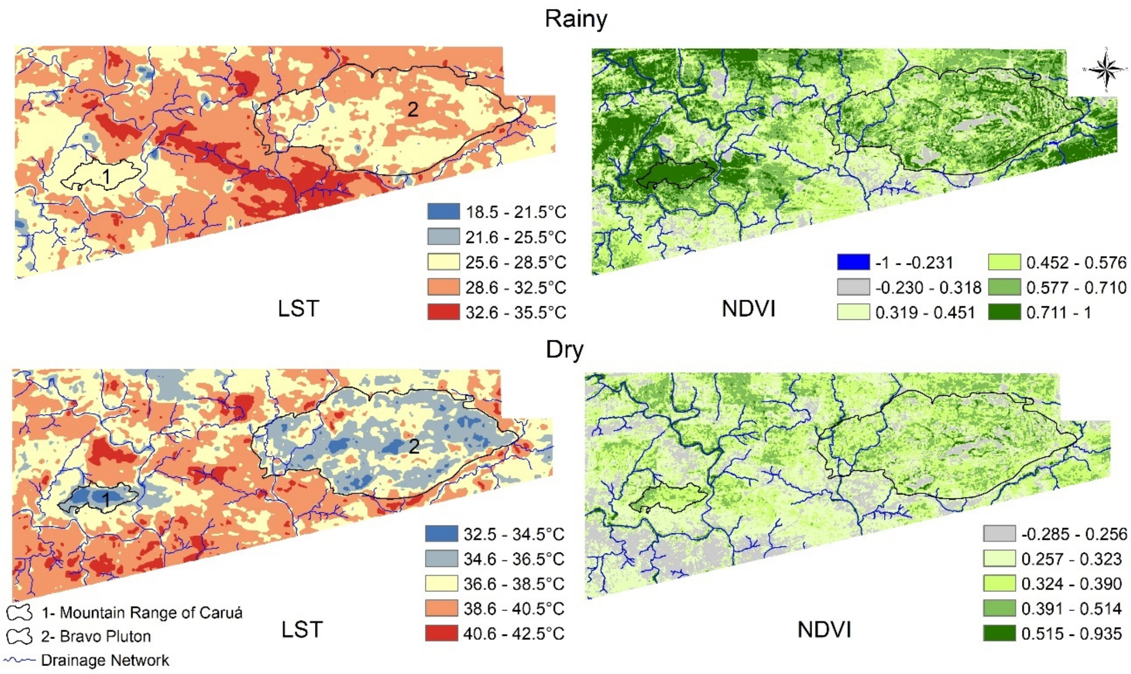

Figure 3. LST and NDVI values.

The LST value calculated for the whole EPA for the month of April (rainy period) varied between 18.5°C and 35.5°C. The NDVI displayed values of -1, relating to water bodies, and 1, indicating the maximum biomass. High levels of water bodies and biomass can be found at this time of year across most of the Cariris Velhos, as February and March are the months of greatest rainfall in the region, with precipitation events extending into July (Medeiros *et al.,* 2015; Silva *et al.,* 2018; Sena *et al.,* 2019).

The rains directly influence the vigour of plant growth, as most of the plants in the Caatinga are deciduous and display rapid leaf renewal during the rainy period (Amorim *et al.,* 2009) due to the availability of more water.

It is important to note that the rains in the Cariri region of Paraíba are not homogeneous and display spatial variability, as well as differences in the volume and time of rainfall (Souza *et al.,* 2009), with a direct impact on the dynamics of the plant cover.

Meanwhile, in October (dry period), the minimum LST value was 32.5°C and the maximum was 42.5°C. The NDVI varied from -0.285, representing areas of exposed soil, to 0.935, the peak biomass recorded, which is most apparent in the few perennial plants growing in the study area. These species are found in more preserved areas such as the Exceptional Areas in the Bravo Pluton and the closed shrubby arboreal Caatinga in the Caruá Mountains, as we will see later.

In the two months prior to October, rainfall tends to decline; August is viewed as a transitional month marking the end of the rainy period, while September has very low or no rainfall in some places. October and November are the driest months of the year (Medeiros *et al.,* 2015; Silva *et al,* 2018; Sena *et al.,* 2019). This can be seen in the rainfall data for 2019, which was obtained from 8 weather stations run by the Executive Agency for Water Management (AESA) of the State of Paraíba (AESA, 2020b) and scattered across the area surrounding the Cariri EPA (Fig. 4).

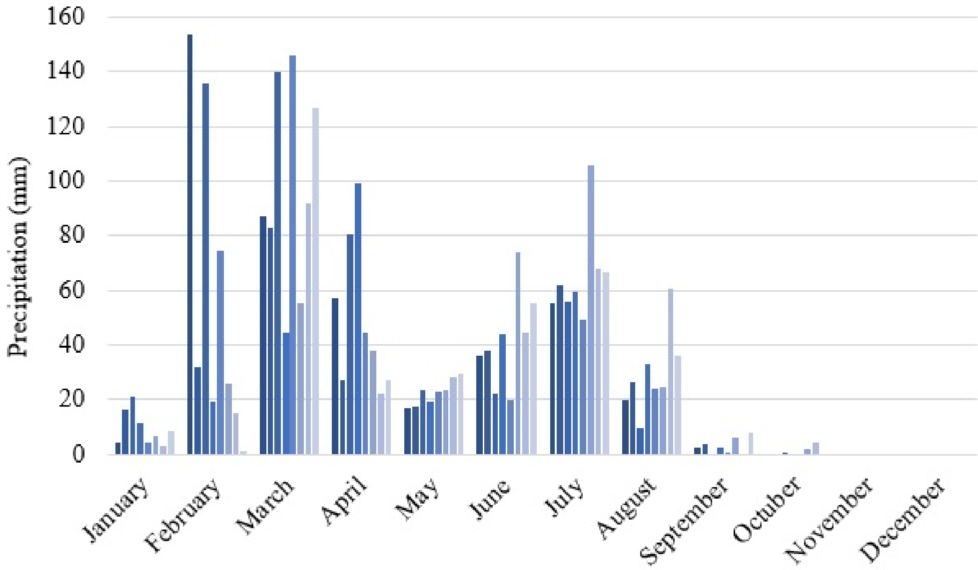

Figure 4. Average monthly rainfall around the Cariri EPA in 2019.

3.2. Soil Surface Moisture Index (SSMI)

The results of the SSMI mapping for April and October 2019 were divided into six categories ranging from 0.0 to 1.0. A result closer to 0.0 indicates that there is less surface moisture, while a result closer to 1.0 suggests a greater concentration of moisture at the surface, according to the scale drawn up by Lopes *et al.* (2011).

By inserting the real validation points (RP) and the points obtained from the images (IP) into the SSMI map (Fig. 5), it was possible to perform a spatial analysis of the points in Desertified Areas and Preserved Areas and link these points to the values for each LST and NDVI category, allowing the interactions between the values for each variable to be observed.

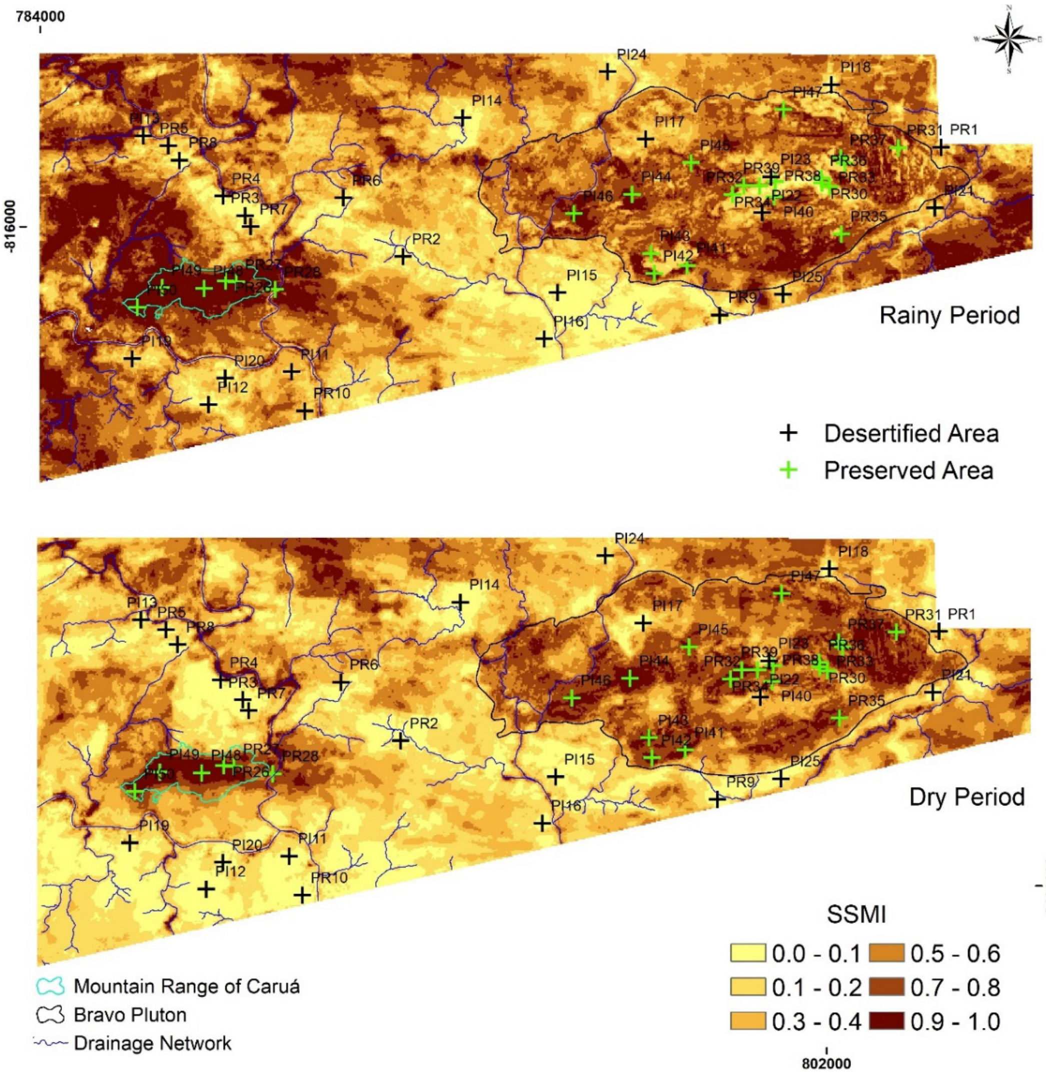

Figure 5. Soil Surface Moisture Index.

The first group of points to be analysed were those relating to Desertified Areas (Fig. 6), which cover large areas as a result of human activity resulting in the intensive removal of native vegetation. These areas are characterised by exposed soils, limited diversity of native plant species contrasting with the presence of exotic species, including mesquite (*Prosopis juliflora*) in particular, and varying degrees of erosion, which is generally advanced (Souza *et al.,* 2015a; Souza and Souza, 2016; Silva *et al.,* 2019a; Araújo and Lima, 2019).

RP.6 - Desertified Area - Rainy Period   RP.3 - Desertified Area - Dry Period

Figure 6. Desertified Areas.

During the rainy period, the points in the Desertified Areas (RP.1-IP.25) fell into the SSMI categories 0.0-0.2 (Table 4), indicating lower concentrations of soil surface moisture. The land surface temperatures (LST) were also high at these points, varying from 28.6 to 35.5°C on the maximum scale calculated for this period, with temperatures of 32.6 - 35.5°C predominating at most of the points. The NDVI ranged from -0.230 (exposed soil) to 0.318 (low density vegetation) at most of the points analysed, and from 0.319 to 0.451 between RP.2, 3 and 6 and IP. 16, 17, 21 and 22, indicating higher levels of biomass but significantly altered vegetation with predominantly exotic species.

Table 4. Relationship between the points and the LST, NDVI and SSMI values for the rainy period.

Point	UTM coord.	Category	LST	NDVI	SSMI
RP.1	804573/9185922	Desertified Area	28.6 - 32.5°C	-0.230 - 0.318	0.1 - 0.2
RP.2	792283/9183321	Desertified Area	32.6 - 35.5°C	0.319 - 0.451	0.0 - 0.1
RP.3	788674/9184254	Desertified Area	32.6 - 35.5°C	0.319 - 0.451	0.0 - 0.1
RP.4	788169/9184906	Desertified Area	32.6 - 35.5°C	-0.230 - 0.318	0.0 - 0.1
RP.5	786917/9185856	Desertified Area	32.6 - 35.5°C	-0.230 - 0.318	0.0 - 0.1
RP.6	790913/9184657	Desertified Area	32.6 - 35.5°C	0.319 - 0.451	0.0 - 0.1
RP.7	788804/9184005	Desertified Area	28.6 - 32.5°C	-0.230 - 0.318	0.1 - 0.2
RP.8	787179/9185522	Desertified Area	32.6 - 35.5°C	-0.230 - 0.318	0.0 - 0.1
RP.9	799512/9181981	Desertified Area	32.6 - 35.5°C	-0.230 - 0.318	0.0 - 0.1
RP.10	790032/9179793	Desertified Area	28.6 - 32.5°C	-0.230 - 0.318	0.1 - 0.2
IP.11	789734/9180685	Desertified Area	28.6 - 32.5°C	-0.230 - 0.318	0.1 - 0.2
IP.12	787841/9179933	Desertified Area	32.6 - 35.5°C	-0.230 - 0.318	0.0 - 0.1
IP.13	786350/9186076	Desertified Area	32.6 - 35.5°C	-0.230 - 0.318	0.0 - 0.1
IP.14	793643/9186488	Desertified Area	32.6 - 35.5°C	-0.230 - 0.318	0.0 - 0.1
IP.15	795813/9182495	Desertified Area	32.6 - 35.5°C	-0.230 - 0.318	0.0 - 0.1
IP.16	795509/9181437	Desertified Area	32.6 - 35.5°C	0.319 - 0.451	0.0 - 0.1
IP.17	797821/9186005	Desertified Area	28.6 - 32.5°C	0.319 - 0.451	0.1 - 0.2
IP.18	802062/9187249	Desertified Area	32.6 - 35.5°C	-0.230 - 0.318	0.0 - 0.1
IP.19	786092/9180985	Desertified Area	32.6 - 35.5°C	-0.230 - 0.318	0.0 - 0.1
IP.20	788216/9180538	Desertified Area	32.6 - 35.5°C	-0.230 - 0.318	0.0 - 0.1
IP.21	804429/9184427	Desertified Area	32.6 - 35.5°C	0.319 - 0.451	0.0 - 0.1
IP.22	800512/9184301	Desertified Area	28.6 - 32.5°C	0.319 - 0.451	0.1 - 0.2
IP.23	800692/9185145	Desertified Area	32.6 - 35.5°C	-0.230 - 0.318	0.0 - 0.1
IP.24	796954/9187546	Desertified Area	32.6 - 35.5°C	-0.230 - 0.318	0.0 - 0.1
IP.25	800962/9182454	Desertified Area	32.6 - 35.5°C	-0.230 - 0.318	0.0 - 0.1

Key: RP=Real points collected in the field; IP=Points collected from the RGB image composition.

The degraded vegetation in the Cariri region in Paraíba is open Caatinga scrubland, where three to four species predominate, usually pioneers with greater resistance to lengthy periods of drought: *pereiro* (*Aspidosperma pyrifolium*); *catingueira* (*Caesalpinia pyramidalis*) and *jurema-preta* (*Mimosa hostilis)*, as well as mesquite (*Prosopis juliflora*), some bromeliads and cacti (Souza *et al.,* 2015b; Bállen *et al.,* 2016; Souza and Souza, 2016; Silva *et al.,* 2019a).

Souza *et al.* (2015b) obtained similar surface temperature values to those observed in this study in their analysis of the end of the rainy period in the upper course of the Paraíba River between 1989 and 2004/2005, with values between 27°C and 35°C for the Cariri EPA. This highlights the issue of the relationship between soil degradation and high ST values in this area.

When analysed during the dry period, the same 25 points displayed an SSMI of only 0.0 to 0.1, as shown in Table 5.

Table 5. Relationship between the points and the LST, NDVI and SSMI values for the dry period.

Point	UTM coord.	Category	LST	NDVI	SSMI
RP.1	804573/9185922	Desertified Area	38.6 - 40.5°C	-0.285 - 0.256	0.0 - 0.1
RP.2	792283/9183321	Desertified Area	38.6 - 40.5°C	-0.285 - 0.256	0.0 - 0.1
RP.3	788674/9184254	Desertified Area	38.6 - 40.5°C	-0.285 - 0.256	0.0 - 0.1
RP.4	788169/9184906	Desertified Area	40.6 - 42.5°C	-0.285 - 0.256	0.0 - 0.1
RP.5	786917/9185856	Desertified Area	38.6 - 40.5°C	-0.285 - 0.256	0.0 - 0.1
RP.6	790913/9184657	Desertified Area	38.6 - 40.5°C	-0.285 - 0.256	0.0 - 0.1
RP.7	788804/9184005	Desertified Area	38.6 - 40.5°C	-0.285 - 0.256	0.0 - 0.1
RP.8	787179/9185522	Desertified Area	38.6 - 40.5°C	-0.285 - 0.256	0.0 - 0.1
RP.9	799512/9181981	Desertified Area	38.6 - 40.5°C	-0.285 - 0.256	0.0 - 0.1
RP.10	790032/9179793	Desertified Area	38.6 - 40.5°C	-0.285 - 0.256	0.0 - 0.1
IP.11	789734/9180685	Desertified Area	38.6 - 40.5°C	-0.285 - 0.256	0.0 - 0.1
IP.12	787841/9179933	Desertified Area	40.6 - 42.5°C	-0.285 - 0.256	0.0 - 0.1
IP.13	786350/9186076	Desertified Area	38.6 - 40.5°C	-0.285 - 0.256	0.0 - 0.1
IP.14	793643/9186488	Desertified Area	40.6 - 42.5°C	-0.285 - 0.256	0.0 - 0.1
IP.15	795813/9182495	Desertified Area	38.6 - 40.5°C	-0.285 - 0.256	0.0 - 0.1
IP.16	795509/9181437	Desertified Area	40.6 - 42.5°C	-0.285 - 0.256	0.0 - 0.1
IP.17	797821/9186005	Desertified Area	40.6 - 42.5°C	-0.285 - 0.256	0.0 - 0.1
IP.18	802062/9187249	Desertified Area	40.6 - 42.5°C	-0.285 - 0.256	0.0 - 0.1
IP.19	786092/9180985	Desertified Area	40.6 - 42.5°C	-0.285 - 0.256	0.0 - 0.1
IP.20	788216/9180538	Desertified Area	40.6 - 42.5°C	-0.285 - 0.256	0.0 - 0.1
IP.21	804429/9184427	Desertified Area	40.6 - 42.5°C	-0.285 - 0.256	0.0 - 0.1
IP.22	800512/9184301	Desertified Area	38.6 - 40.5°C	-0.285 - 0.256	0.0 - 0.1
IP.23	800692/9185145	Desertified Area	38.6 - 40.5°C	-0.285 - 0.256	0.0 - 0.1
IP.24	796954/9187546	Desertified Area	40.6 - 42.5°C	-0.285 - 0.256	0.0 - 0.1
IP.25	800962/9182454	Desertified Area	40.6 - 42.5°C	-0.285 - 0.256	0.0 - 0.1

Key: RP=Real points collected in the field; IP=Points collected from the RGB image composition.

In this case, all 25 points displayed the highest LST levels calculated, ranging from 38.6°C to 42.5°C, with an NDVI varying from -0.285 to 0.256, with negative values indicating areas of exposed soil (-0.285) and positive values suggesting low levels of biomass. At points where the NDVI values were higher than in the rainy period (0.319 - 0.451), such as RP.2, 3, 6 and IP.16, 17, 21 and 22, positive biomass values were observed in the dry period; however, in the case of the latter, these values did not exceed 0.256, indicating a degree of biomass in the areas occupied by pioneer plants and mesquite.

The LST for these points followed a similar pattern to that observed during the rainy period, with higher levels displayed. IP.17 was an exception, scoring the second highest ST (28.6 - 32.5°C) and an SSMI of 0.1-0.2 in the rainy period and the maximum LST value (40.6 to 42.5°C) and the minimum SSMI (0.0 – 0.1) in the dry period.

In this regard, the points obtained in the field and from the images for the Desertified Areas analysed display very similar patterns when the LST, NDVI and SSMI values for the rainy and dry periods are compared. These patterns are shaped by a high LST and a low NDVI or no biomass, resulting in a low SSMI, which is indicative of drier areas owing largely to the process of degradation.

Especially during rainy periods, high surface temperatures and low levels of biomass in areas potentially degraded by desertification are a warning sign, revealing the difficulty of spontaneous regeneration of the native vegetation in the Caatinga since the process of seed germination for most of the plants in this biome occurs primarily during this period (Souza *et al.,* 2015b).

According to Lemos *et al.* (2020), the rising surface temperatures caused primarily by the removal of native vegetation result in high exposure of the soil to solar radiation, hindering the germination of seeds from the different plant species, as this process depends on a certain temperature in order to be able to occur, thus obstructing the ecological succession as a result of changes to part of the system. Like other tropical and sub-tropical biomes, ideal temperatures in the Caatinga are considered to lie between 20 and 30ºC (Carvalho and Nakagawa, 2000).

These areas degraded by desertification are located on gently undulating and flat terrain, usually close to the drainage network (Silva *et al.,* 2019a), and are the result of human activity linked to forms of land use which have been practised since settlement began in the region in the 17th century. Deforestation of native vegetation began with the introduction of farming activities, with a second, more intense period resulting from cotton cultivation between the 19th century and the mid-1980s (Souza *et al.,* 2015a).

More recently, in the 1970s, further changes to the landscape of Cariri occurred with the introduction of exotic tree species such as mesquite by the Federal Government to provide an economic alternative for the region. The species serves as feed for livestock and led to intensifying deforestation of the remaining native vegetation to make room for cultivation (Souza *et al.,* 2015a), with a negative environmental impact. Fuel is also extracted as a source of energy for making fences and structures for homes (Travassos and Souza, 2014).

It is noteworthy that even in areas where mesquite predominates, indicating slightly higher biomass values, especially in the dry period, they do not have similar characteristics to the Preserved Areas or the same ecological features, as they do not present plant diversity of native species, being mesquite extremely competitive and which makes it predominant over other plant species. And because they are very resistant to long periods of drought and endowed with biomass, they also end up influencing human action in their introduction in a disorderly way. Thus, configuring another type of environmental degradation favoring the desertification process.

The analysis was extended into the Preserved Areas in the EPA, using another 25 points (RP.26 to IP.50). These areas were dominated by two main types of plant formation: shrubby arboreal Caatinga and Exceptional Areas.

Shrubby arboreal Caatinga (Fig. 7) is characterised by a greater, denser presence of trees. This type of vegetation was mostly identified in an area of higher altitude, the Caruá Mountains located in the southwest of the EPA. Meanwhile, the Exceptional Areas can be found in areas located near the large rocky outcrops (*lajedos*) in the Bravo Pluton region (Souza and Souza, 2016; Silva *et al.,* 2019a; Silva *et al.,* 2019b).

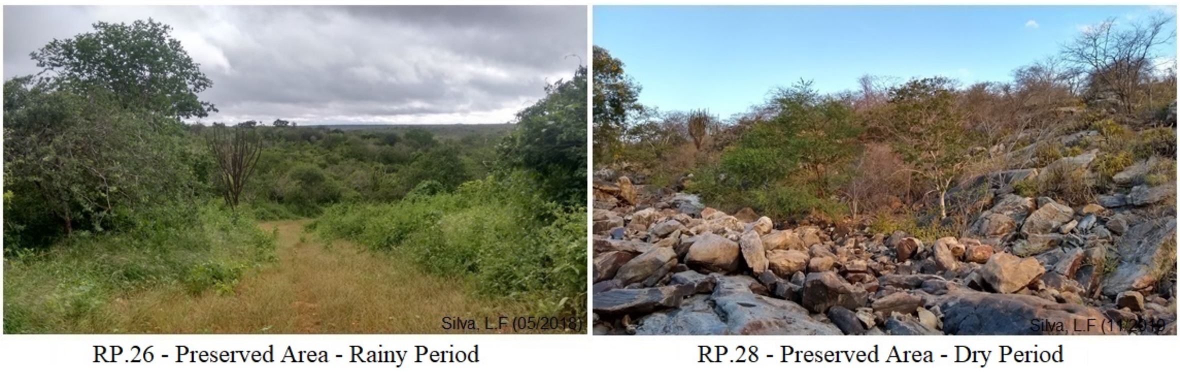

Figure 7. Preserved Area - Shrubby arboreal Caatinga.

The Exceptional Areas in the Cariri EPA (Fig. 8) occupy narrow strips between the *lajedos* of Bravo Pluton measuring approximately 10 to 20 metres wide. They are largely made up of tree species, many of which belong to other Brazilian biomes, including Amazon, Cerrado and Atlantic Forest, where higher rainfall and moisture levels are found (Lunguinho *et al.,* 2015; Silva *et al.,* 2019b), mixed with typical species from the Caatinga commonly found in riverside areas. Therefore, the presence of these species indicates higher moisture levels at the local level.

RP.34 - Preserved Area - Rainy Period RP.32 - Preserved Area - Dry Period

Figure 8. Preserved Area - Exceptional Areas.

During the rainy period, the SSMI values identified at the points in these areas were the highest in the EPA, oscillating between 0.7 and 1.0 (Table 6) and indicating high levels of soil surface moisture.

Table 6. Relationship between the points and the LST, NDVI and SSMI values for the rainy period.

Point	UTM coord.	Category	LST	NDVI	SSMI
RP.26	788235/9182755	Shrub.Arbo.Caat.	25.6 - 28.5°C	0.711 - 1	0.9 - 1.0
RP.27	788475/9182734	Shrub.Arbo.Caat.	25.6 - 28.5°C	0.711 - 1	0.9 - 1.0
RP.28	788363/9182567	Shrub.Arbo.Caat.	25.6 - 28.5°C	0.577 – 0.710	0.9 - 1.0
RP.29	802368/9185462	Exceptional Areas	28.6 - 32.5°C	0.711 - 1	0.7 - 0.8
RP.30	801848/9185002	Exceptional Areas	28.6 - 32.5°C	0.711 - 1	0.7 - 0.8
RP.31	803593/9185805	Exceptional Areas	25.6 - 28.5°C	0.711 - 1	0.9 - 1.0
RP.32	799812/9184732	Exceptional Areas	25.6 - 28.5°C	0.711 - 1	0.9 - 1.0
RP.33	802026/9184919	Exceptional Areas	28.6 - 32.5°C	0.711 - 1	0.7 - 0.8
RP.34	800425/9184939	Exceptional Areas	28.6 - 32.5°C	0.711 - 1	0.7 - 0.8
RP.35	802298/9183836	Exceptional Areas	25.6 - 28.5°C	0.711 - 1	0.9 - 1.0
RP.36	801832/9185110	Exceptional Areas	25.6 - 28.5°C	0.711 - 1	0.9 - 1.0
RP.37	802283/9185583	Exceptional Areas	25.6 - 28.5°C	0.711 - 1	0.9 - 1.0
RP.38	800788/9185034	Exceptional Areas	28.6 - 32.5°C	0.711 - 1	0.7 - 0.8
RP.39	800065/9184941	Exceptional Areas	25.6 - 28.5°C	0.711 - 1	0.9 - 1.0
IP.40	800760/9184679	Exceptional Areas	28.6 - 32.5°C	0.711 - 1	0.7 - 0.8
IP.41	798775/9183112	Exceptional Areas	25.6 - 28.5°C	0.711 - 1	0.9 - 1.0
IP.42	798018/9182933	Exceptional Areas	25.6 - 28.5°C	0.711 - 1	0.9 - 1.0
IP.43	797945/9183390	Exceptional Areas	25.6 - 28.5°C	0.711 - 1	0.9 - 1.0
IP.44	797515/9184745	Exceptional Areas	25.6 - 28.5°C	0.711 - 1	0.9 - 1.0
IP.45	798861/9185463	Exceptional Areas	25.6 - 28.5°C	0.711 - 1	0.9 - 1.0
IP.46	796185/9184299	Exceptional Areas	25.6 - 28.5°C	0.577 – 0.710	0.7 - 0.8
IP.47	800974/9186686	Exceptional Areas	25.6 - 28.5°C	0.577 – 0.710	0.7 - 0.8
IP.48	787737/9182588	Shrub.Arbo.Caat.	25.6 - 28.5°C	0.711 - 1	0.9 - 1.0
IP.49	786774/9182608	Shrub.Arbo.Caat.	25.6 - 28.5°C	0.711 - 1	0.9 - 1.0
IP.50	786217/9182160	Shrub.Arbo.Caat.	25.6 - 28.5°C	0.711 - 1	0.9 - 1.0

Key: RP = Real points collected in the field; IP = Points collected from the RGB image composition; Shrub. Arbo.Caat. = Shrubby arboreal Caatinga.

In these areas, the surface temperature varied from 25.6 to 32.5°C, with temperatures of 25.6 to 28.5°C predominant at most points and especially in the areas of shrubby arboreal Caatinga, where this LST value was found at every point. In the Exceptional Areas, at points RP.29, 30, 33, 34, 38 and IP.40, the ST was higher, ranging from 28.6 - 32.5°C. This is due to the fact that these points are located in more open areas of vegetation, which are influenced by smaller, more widely spaced *lajedos*.

Most of the points analysed displayed an NDVI of 0.711 - 1, with lower values found only at RP.28 and IP.46 and 47 (0.577 – 0.710), which are located in areas with a greater presence of dense arboreal Caatinga (another common vegetation type in the region) on steeper slopes in the Caruá Mountains and between the *lajedos* of Bravo Pluton.

During the rainy period, the vast majority of the points analysed in both Preserved Areas saw LST values below 30°C, while temperatures did not exceed 32°C at the other points in these areas. Echoing the findings of Carvalho and Nakagawa (2000) and Souza *et al.* (2015b), these areas are characterised by improved conditions for germination for the majority of the Caatinga plant species compared to areas with a higher LST, such as the Desertified Areas, especially during the rainy period, where there is an expansion of biomass and greater retention of soil surface moisture due to the availability of water and the type of vegetation found in these areas.

Confirming this observation, during the dry period, the 25 points analysed (RP.26 to IP.50) also had an SSMI of 0.7 - 1.0, indicating that there was a high concentration of soil surface moisture at these locations, as Table 7 shows.

Table 7. Relationship between the points and the LST, NDVI and SSMI values for the dry period.

Point	UTM coord.	Category	LST	NDVI	SSMI
RP.26	788235/9182755	Shrub.Arbo.Caat.	32.5 - 34.5°C	0.324 - 0.390	0.9 - 1.0
RP.27	788475/9182734	Shrub.Arbo.Caat.	34.6 - 36.5°C	0.324 - 0.390	0.9 - 1.0
RP.28	788363/9182567	Shrub.Arbo.Caat.	32.5 - 34.5°C	0.324 - 0.390	0.7 - 0.8
RP.29	802368/9185462	Exceptional Areas	34.6 - 36.5°C	0.391 - 0.514	0.9 - 1.0
RP.30	801848/9185002	Exceptional Areas	34.6 - 36.5°C	0.515 - 0.935	0.9 - 1.0
RP.31	803593/9185805	Exceptional Areas	32.5 - 34.5°C	0.515 - 0.935	0.9 - 1.0
RP.32	799812/9184732	Exceptional Areas	32.5 - 34.5°C	0.391 - 0.514	0.9 - 1.0
RP.33	802026/9184919	Exceptional Areas	34.6 - 36.5°C	0.515 - 0.935	0.9 - 1.0
RP.34	800425/9184939	Exceptional Areas	34.6 - 36.5°C	0.515 - 0.935	0.9 - 1.0
RP.35	802298/9183836	Exceptional Areas	34.6 - 36.5°C	0.515 - 0.935	0.9 - 1.0
RP.36	801832/9185110	Exceptional Areas	34.6 - 36.5°C	0.515 - 0.935	0.9 - 1.0
RP.37	802283/9185583	Exceptional Areas	32.5 - 34.5°C	0.515 - 0.935	0.9 - 1.0
RP.38	800788/9185034	Exceptional Areas	34.6 - 36.5°C	0.515 - 0.935	0.9 - 1.0
RP.39	800065/9184941	Exceptional Areas	32.5 - 34.5°C	0.515 - 0.935	0.9 - 1.0
IP.40	800760/9184679	Exceptional Areas	34.6 - 36.5°C	0.515 - 0.935	0.9 - 1.0
IP.41	798775/9183112	Exceptional Areas	32.5 - 34.5°C	0.515 - 0.935	0.9 - 1.0
IP.42	798018/9182933	Exceptional Areas	32.5 - 34.5°C	0.515 - 0.935	0.9 - 1.0
IP.43	797945/9183390	Exceptional Areas	34.6 - 36.5°C	0.515 - 0.935	0.9 - 1.0
IP.44	797515/9184745	Exceptional Areas	32.5 - 34.5°C	0.391 - 0.514	0.9 - 1.0
IP.45	798861/9185463	Exceptional Areas	34.6 - 36.5°C	0.515 - 0.935	0.9 - 1.0
IP.46	796185/9184299	Exceptional Areas	34.6 - 36.5°C	0.391 - 0.514	0.7 - 0.8
IP.47	800974/9186686	Exceptional Areas	34.6 - 36.5°C	0.391 - 0.514	0.9 - 1.0
IP.48	787737/9182588	Shrub.Arbo.Caat.	32.5 - 34.5°C	0.391 - 0.514	0.9 - 1.0
IP.49	786774/9182608	Shrub.Arbo.Caat.	32.5 - 34.5°C	0.391 - 0.514	0.9 - 1.0
IP.50	786217/9182160	Shrub.Arbo.Caat.	34.6 - 36.5°C	0.391 - 0.514	0.9 - 1.0

Key: RP = Real points collected in the field; IP = Points collected from the RGB image composition; Shrub. Arbo.Caat. = Shrubby arboreal Caatinga.

The LST values ranged from 32.5 to 36.5°C, representing the lowest level calculated for this period. Moreover, the NDVI varied from 0.324 to 0.935, indicating high levels of biomass at most of the points during this period of the year, especially in the Exceptional Areas, as shown in Table 4.

In the points relating to areas of shrubby arboreal Caatinga, the NDVI oscillated between 0.324 and 0.390 in areas located on the slopes of the Caruá Mountains, where the dominant vegetation is Caatinga scrubland, and from 0.391 to 0.514 at the highest points in this area, IP.48, 49 and 50, where the phytophysiognomy is still denser and more arboreal.

In the Exceptional Areas, some points displayed an NDVI ranging between 0.391 and 0.514, such as RP.29 and 32 and IP.44, 46 and 47, where closed Caatinga scrubland is more dominant. However, the remaining points in this area had biomass values between 0.515 and 0.935, located in strips around the *lajedos* of Bravo Pluton. These areas of high biomass are clearly visible during the dry period in the region (Figure 6), when many evergreen species can maintain themselves due to higher local moisture levels. In the more distant Bravo Pluton area, the predominant vegetation is open shrubby Caatinga, usually deciduous.

Comparing the rainy and dry periods for these points in Preserved Areas, the SSMI and NDVI were high in both and only the LST varied. The lowest temperature values were found in the dry period, while moderate temperatures ranging from 25.5 to 28.0ºC were observed in the rainy period at most points, with the exception of more open areas where maximum temperatures of 32.5°C were found.

In our understanding, these factors are only possible in these areas due to the presence of certain specific natural characteristics: in the case of shrubby arboreal Caatinga, the relative altitude of the mountains is linked to low local levels of anthropisation, while in the Exceptional Areas, the geological and geomorphological conditions generated by the large rocky outcrops in the Bravo Pluton encourage the concentration of moisture. In the latter case in particular, a kind of micro-environment with unique characteristics develops, contrasting with its surroundings in terms of soil type, moisture retention and nutrient availability, as well as soil and air temperature, shade and other important conditions that make these places conducive to vigorous growth of the species colonising them (Lunguinho *et al.,* 2015; Silva *et al.,* 2019b).

It is also relevant to note that conservation of the plant cover is facilitated in these areas by the conditions imposed by the topography and geomorphology, making it difficult for human activities making more direct, impactful use of the land to take place. This is the case of the Caruá Mountains, due to their striking topographic relief, and the Bravo Pluton, due to the presence of large rocky outcrops.

4. Conclusions

Combining the points used with the biophysical and geophysical data captured by orbital sensors enabled two different types of environmental conditions to be identified and described and a number of highly relevant characteristics to be observed regarding the two categories analysed in this study.

In Desertified Areas, factors such as a higher surface temperature, low levels of biomass and low soil surface moisture are present throughout the year, although they are exacerbated by the dry period.

Analysis of the points linked to the Preserved Areas revealed the presence of factors that were more conducive to the balance and maintenance of plant cover, with high levels of biomass and a concentration of surface moisture, as well as surface temperatures sufficient for seed germination in the rainy period and lower temperatures than other areas during the dry period.

These results may be combined with other information as part of the management process and search for mitigation measures in degraded areas, especially those areas suffering desertification in semi-arid regions. In the case of Conservation Units like the Cariri EPA, the methodology employed in this study may be used to inform land-use management plans and, more broadly, to plan a more rational use of the natural resources available in biomass like that found in the Caatinga and other biomes with a similar climate.

Acknowledgements

The first author is grateful to CAPES/Brazil for the PhD scholarship awarded via FAPESQ, Public Notice no. 003/2016, Case no. 88887.369009/2019-00, and to the Postgraduate Programme in Geography at the Federal University of Paraíba in Brazil.

References

AESA (Agência Executiva de Gestão das Águas do Estado da Paraíba), 2020a. Bacia Hidrográfica do Rio Paraíba. Available in: http://www.aesa.pb.gov.br/aesa-website/comite-de-bacias/rio-paraiba/

AESA (Agência Executiva de Gestão das Águas do Estado da Paraíba), 2020b Meteorologia – Chuvas. Available in: http://www.aesa.pb.gov.br/aesa-website/meteorologia-chuvas/

Amorim, I. L., Sampaio, E.V.S.B., Araújo, E. L., 2009. Fenologia de espécies lenhosas da caatinga do Seridó, RN. *Revista Árvore* 33(3), 491-499. Available in: https://www.scielo.br/pdf/rarv/v33n3/11.pdf

Aquino, C.M.S., Almeida, J.A.P., Oliveira, J.G.B. 2012. Estudo da cobertura vegetal/uso da terra nos anos de 1987 e 2007 no núcleo de degradação/desertificação de São Raimundo Nonato – Piauí. *Revista RA´EGA o Espaço Geográfico em Análise* 25, 252-278. https://doi.org/10.5380/raega.v25i0.28013

Aráujo, S.M.S., Lima, E.R.V., 2019. Semiárido Brasileiro e Desertificação. In Araújo, S.M.S. and Lima, E.R.V. (Coord.), *Desertificação no semiárido brasileiro e paraibano abordagens conceituais, metodologias e indicadores,* pp. 55-62, Bahia: Paulo Afonso. Available in: http://www.sabeh.org.br/?mbdb_book=desertificacao-no-semiarido-brasileiro-e-paraibano

Ballén, L.A.C., Souza, B.I., Lima, E.R.V., 2016. Análise espaço-temporal da cobertura vegetal na área de proteção ambiental do Cariri, Paraíba, Brasil. *Boletim Goiano de Geografia* 36(3), 55-571. https://doi.org/10.5216/bgg.v36i3.44558

Bezerra, F.G.S., Aguiar, A.P.D., Alvalá, R.C., Giarolla, A., Bezerra, K.R.A., Lima, P.V.P.S., Nascimento, F.R., Arai, E. 2020. Analysis of areas undergoing desertification, using EVI2 multi-temporal data based on MODIS imagery as indicator. *Ecological Indicators* 117, 01-15. https://doi.org/10.1016/j.ecolind.2020.106579

Carvalho, N., Nakagawa, M., 2000. *Sementes: ciência, tecnologia e produção.* 4ª ed. Jaboticabal: FUNEP.

Castelletti, C.H.M., Santos, A.M.M., Tabarelli M., Silva, J.M.C., 2003. Quanto ainda resta da Caatinga? In: *Ecologia e conservação da Caatinga*. Editora Universitária da UFPE, pp. 719-734, Recife.

Conti, J.B. 2007. *Clima e meio ambiente.* Atual. São Paulo.

Francisco, P.R.M., Chaves, I.B., Chaves, L.H.G., Lima, E.R.V., Silva, B.B. 2017. Umidade antecedente e índice de vegetação da diferença normalizada no mapeamento da Caatinga. *Agropecuária Científica no Semiárido* 13(2), 82-91. http://revistas.ufcg.edu.br/acsa/index.php/ACSA/index

Inocêncio, T.M., Neto, A.R., Souza, A.G.S.S. 2020. Soil moisture obtained through remote sensing to assess drought events. *Revista Brasileira de Engenharia Agrícola e Ambiental* 24(9), 575-580. http://doi.org/10.1590/1807-1929/agriambi.v24n9p575-580

INSA (INSTITUTO NACIONAL DO SEMIÁRIDO), 2015. *Relatórios. Relatório do seminário nacional combate à desertificação, degradação das terras e convivência com a semiaridez para redução da pobreza e um desenvolvimento sustentável.* Instituto Nacional do Semiárido. Departamento de Combate à Dertificaçao, FAO, Instituto Interamericano de Cooperaçao para Agricultura.

Köppen, W.P. 1931. *Grundriss der Klimakunde.* Walter de Gruyter. Berlín. Available in: https://www.worldcat.org/title/grundriss-der-klimakunde/oclc/2549942

Lages, G.A. Marinho, M.S., Nascimento, M.A.L., Medeiros, V.C., Dantas, E.L. Fialho, D., 2013. Mar de Bolas do Lajedo do Pai Mateus, Cabaceiras, PB - Campo de matacões graníticos gigantes e registros rupestres de civilização pré-colombiana. *In*: Winge, M., Schobbenhaus, C., Souza, C.R.G., Fernandes, A.C.S., Berbert-Born,M., Sallun Filho, W., Queiroz, E.T. (Edit.). *Sítios Geológicos e Paleontológicos do Brasil.* Available in: http://sigep.cprm.gov.br/sitio068/sitio068.pdf

Lemos, J.E., Souza, B.I., Diniz, M.T.M., 2020. Sistemas, caos e o processo de desertificação no semiárido brasileiro: complexidade e interações. *Ateliê Geográfico* 14(01), 136-154. https://doi.org/10.5216/ag.v14i1.57004

Lima, F.S., Almeida, N.V., 2017. Dinâmica espaço-temporal da cobertura vegetal na Área de Proteção Ambiental (APA) do Cariri, Paraíba-PB, Brasil. *Revista Brasileira de Geografia Física* 10(3), 699-721. https://doi.org/10.5935/1984-2295.20170046

Lopes, H.L., Accioly, L.J.O., Silva, F.H.B.B., Sobral, M.C.M., Araújo Filho, J.C., Candeias, A.L.B., 2011. Espacialização da umidade do solo por meio da temperatura da superfície e índice de vegetação. *Revista Brasileira de Engenharia Agrícola e Ambiental* 15(09) 973-980. https://doi.org/10.1590/S1415-43662011000900014

Lunguinho, R.L., Souza, B.I., Queiroz, R.T., Cardoso, E.C.M.A. 2015. Influência dos lajedos na composição florística do seu entorno, no sítio Salambaia – Cabaceiras – PB. *Revista Equador* 4(3), 230-237. Available in: https://revistas.ufpi.br/index.php/equador/article/view/3643/2119

Medeiros, R.M., Santos, D.C., Francisco, P.R.M., Gomes Filho, M.F., 2015. Análise hidroclimática da região de São João Do Cariri-PB. *Revista Educação Agrícola Superior* 30(2), 59-65.

Melo, M.L. 1988. *Áreas de exceção da Paraíba e dos sertões de Pernambuco*. SUDENE. Recife, 8 pp.

Mello Neto, A.V. de, Lins, R.C., Coutinho, S.F.S., 1985. Áreas de exceção do Nordeste brasileiro considerações conceituais. In: *SUDENE, Fundação Joaquim Nabuco - Áreas de exceção do Nordeste (Coord). Pernambuco e Paraíba*, pp. 1-11. Recife. Available in: http://observatoriogeograficoamericalatina.org.mx/egal3/Geografiasocioeconomica/Geografiaagricola/01.pdf

MMAUC (Ministério do Meio Ambiente. Unidades de Conservação), 2020. Available in: https://www.gov.br/mma/pt-br

MMA (Ministério do Meio Ambiente), 2020. In *Programa de Ação Nacional de Combate à Desertificação e Mitigação dos Efeitos da Seca PAN-Brasil*. Available in: https://www.gov.br/mma/pt-br

MTERD (Ministerio para la Transición Ecológica y Reto Demográfico), 2020. Available in: https://www.miteco.gob.es/es/biodiversidad/legislacion/legislacion-y-convenios/convenios-internacionales/convencion_desertificacion.aspx

Nascimento, F.R., 2015. Os semiáridos e a desertificação no Brasil. REDE-*Revista Eletrônica do PRODEMA* 9(2), 7–26.

Portillo-Quintero, C.A., Sánchez-Azofeifa, G.A., 2010. Extent and conservation of tropical dry forests in the Americas. *Biological Conservation* 143(1), 144-155. https://doi.org/10.1016/j.biocon.2009.09.020

Rouse, J.W., Haas, R.H., Schell, J.A., Deering, D.W., 1973. Monitoring vegetation systems in the Great Plains with ERTS. *NTRS – NASA Technical Reports Server.* 1, 309-317. Available in: https://ntrs.nasa.gov/api/citations/19740022614/downloads/19740022614.pdf

Romano, M.P.C.G., Rocha, J.G., Santos, M.L.F., Souza, M.C.S., 2018. Unidades paisagísticas no semiárido paraibano: porção Leste do Plúton Bravo, Cabaceiras-PB. In: Plataforma Espaço digital (pp. 1-10). Actas del II Congresso Internacional Da Diversidade Do Semiárido. Paraíba, novembro 8-10 de 2017. Available in: http://www.editorarealize.com.br/index.php/artigo/visualizar/33912

Santos, C.V.B., Carvalho, H.F.S., Silva, M.J., Moura, M.S.B., Galvíncio, J.D., 2020. Uso de sensoriamento remoto na análise da temperatura da superfície em áreas de floresta tropical sazonalmente seca. *Revista Brasileira de Geografia Física* 13(03), 941-953. https://doi.org/10.26848/rbgf.v13.3.p941-957

Sena, J.P.O., Moraes Neto, J.M., Lucena, D.B., 2019. Variabilidade da precipitação em Sumé e São João do Cariri e suas consequências na agropecuária. *Revista Brasileira de Climatologia* 25**,** 278-293. http://doi.org/10.5380/abclima.v25i0.65182

Silva, G.S., Silva, W.S., Silva, A.L., Almeida, N.V., Araújo, L.E., 2018. Análise da precipitação da microrregião do Cariri oriental paraibano. *Revista REGNE* 4(1), 42-57. Available in: https://periodicos.ufrn.br/revistadoregne/article/view/13938

Silva, L.F., Souza, B.I., Bacani, V.M., 2019a. Intensidade da ação antrópica na área de proteção ambiental do Cariri paraibano. *Caminhos de Geografia* 20(71), 364-383.

Silva, L.F., Souza, B.I., Bacani, V.M., 2019b. Desempenho comparativo entre classificadores supervisionados no mapeamento de áreas de Ecótono em região de Caatinga. *Caderno de Geografia* 29(59), 1083-1105. https://doi.org/10.5752/P.2318-2962.2019v29n59p1083

Silva Filho, R., Vasconcelos, R.S., Galvão, C.O., Rufino, I.A.A., Cunha, E.B.L., 2020. Representação matemática do comportamento intra-anual do NDVI no bioma Caatinga. *Ciência Florestal* 30(2), 473-488. https://doi.org/10.5902/1980509837279

Sobrinho, J.V., 1982. *Processos de desertificação no Nordeste do Brasil: sua gênese e sua contenção*. Sudene, 101 pp., Recife.

Sousa, F.P., Ferreira, T.O., Mendonça, E.S., Romero, R.E., Oliveira, J.G.B., 2012. Carbon and nitrogen in degraded Brazilian semi-arid soils undergoing desertification. *Agriculture, Ecosystems and Environment*, 148, 11-21. https://doi.org/10.1016/j.agee.2011.11.009

Souza, B.I., Suertegaray, D.M.A., Lima, E. R.V., 2009. Desertificação e seus efeitos na vegetação e solos do Cariri Paraibano. *Mercator* 8(16), 217-232. Available in: http://www.mercator.ufc.br/mercator/article/view/250

Souza, B.I., Queiroz, R.T., Cardoso, E.C.M., 2015a. Degradação e riscos à desertificação no alto curso do rio Paraíba – PB/Brasil. *Revista da Associação Nacional de Pós-graduação e Pesquisa em Geografia (Anpege)* 11(16), 201-222. https://doi.org/10.5418/RA2015.1116.0009

Souza, B.I. Macêdo, L.A., Silva, G.J.F., 2015b. Temperatura dos solos e suas influências na regeneração natural da Caatinga nos Cariris Velhos – PB. *Revista RA'EGA* 35, 261-287. http://doi.org/10.5380/raega.v35i0.41609

Souza, B.I., Souza, R.S., 2016. Processo de ocupação dos Cariris Velhos – PB e efeitos na cobertura vegetal: contribuição à Biogeografia Cultural do semiárido. *Caderno de Geografia* 26(2) 229-258. https://doi.org/10.5752/p.2318-2962.2016v26nesp2p229

Souza, N.R.L., Xavier, R.A., 2017. A importância dos "lajedos" na paisagem geomorfológica do Cariri Paraibano. In: Os desafios da Geografia Física na Fronteira do Conhecimento. Actas del XVII Simpósio Brasileiro De Geografia Física Aplicada. Campinas, june 28-30 and 02 july, pp. 6561-6566. Available in: https://www.researchgate.net/publication/321304297_A_importancia_dos_lajedos_na_paisagem_geomorfologica_do_Cariri_Paraibano

Travassos, I.S., Souza, B.I., 2014. Desmatamento e Desertificação no Cariri Paraibano. *Revista Brasileira de Geografia Física* 07(1), 103-116. https://periodicos.ufpe.br/revistas/rbgfe/article/viewFile/232905/26887

Vieira, R.M.S.P., Sestini, M.F., Tomasella, J., Marchezini, V., Pereira, G.R., Barbosa, A.A., Santos, F.C., Rodriguez, D.A., Nascimento, F.R., Santana, M. O., Campello, F.B. C., Ometto, J.P.H., 2020. Characterizing spatio-temporal patterns of social vulnerability to droughts, degradation and desertification in the Brazilian northeast. *Environmental and Sustainability Indicators* 5, 01-09. https://doi.org/10.1016/j.indic.2019.100016

Wang, H., Li, X., Long, H., Xu, X., Bao, Y., 2010. Monitoring the effects of land use and cover type changes on soil moisture using remote-sensing data: A case study in China's Yongding River basin. *Catena* 82, 135-145. https://doi.org/10.1016/j.catena.2010.05.008

Zhan, Z., Qin, Q., Wang, X., 2004. The application of LST/NDVI index for monitoring land surface moisture in semiarid area. *IEEE Transactions on geosciences and Remote Sensing* 3, 1551-1554. https://doi.org/10.1109/IGARSS.2004.1370609

Zhou, W., Gang, C., Zhou, F., Li, J., Dong, X., Zhao, C., 2015. Quantitative assessment of the individual contribution of climate and human factors to desertification in northwest China using net primary productivity as an indicator. *Ecological Indicators* 48, 560-569. https://doi.org/10.1016/j.ecolind.2014.08.043